Accepted Manuscript

Stress response to high osmolarity in *Trypanosoma cruzi* epimastigotes

Sergio Bonansea, Melina Usorach, María Celeste Gesumaría, Verónica Santander, Alba Marina Gimenez, Mariana Bollo, Estela Machado
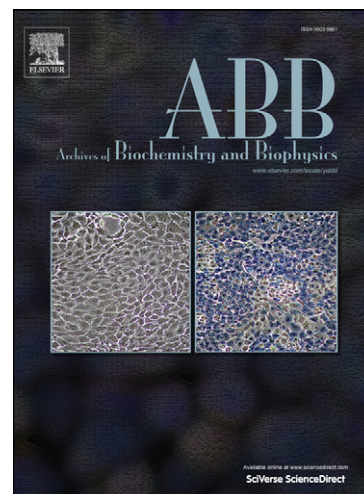
Please cite this article as: S. Bonansea, M. Usorach, a.C. Gesumaría, V. Santander, A.M. Gimenez, M. Bollo, E. Machado, Stress response to high osmolarity in *Trypanosoma cruzi* epimastigotes, *Archives of Biochemistry and Biophysics* (2012), doi: http://dx.doi.org/10.1016/j.abb.2012.07.014

1   Stress response to high osmolarity in *Trypanosoma cruzi* epimastigotes

2   Sergio Bonansea†, Melina Usorach†, María Celeste Gesumaría, Verónica Santander,

3   Alba Marina Gimenez, Mariana Bollo[2] and Estela Machado[1].

4   *Química biológica, Facultad de Ciencias Exactas, Físico-Químicas y Naturales.*

5   *Universidad Nacional de Río Cuarto, 5800 Río Cuarto, Córdoba, Argentina.*

6

7   [1] To whom correspondence should be addressed. Estela Machado, Química Biológica,

8   FCEFQN, UNRC. 5800 Río Cuarto, Córdoba, Argentina.

9   Phone: 0054-358-4676424 Fax: 0054-358-4676232

10   *E-mail*: emachado@exa.unrc.edu.ar

11   †These authors contributed equally to this work.

12   [2]Present address, Instituto de Investigación Médica Mercedes y Martín Ferreyra.

13   CONICET. Córdoba, Argentina.

14

15

16

17

18

19

20

21

22

23

24

25

26

27

28

29

30

31

32

33

34

Abstract

Trypanosoma cruzi undergoes differentiation in the rectum of triatomine, where increased osmolarity is caused mainly by elevated content of NaCl from urine. Early biochemical events in response to high osmolarity in this parasite have not been totally elucidated. In order to clarify the relationship between these events and developmental stages of *T. cruzi*, epimastigotes were subjected to hyperosmotic stress, which caused activation of Na^+/H^+ exchanger from acidic vacuoles and accumulation of inositol trisphosphate ($InsP_3$). Suppression of $InsP_3$ levels was observed in presence of intracellular Ca^{2+} chelator or pre-treatment with 5-(N-ethyl-N-isopropyl)-amiloride (EIPA), which also inhibited the alkalinization of acidic vacuoles via a Na^+/H^+ exchanger and the consequent increase in cytosolic calcium. These effects were activated and inhibited by PMA and Chelerythrine respectively, suggesting regulation by protein kinase C. The *T. cruzi* Na^+/H^+ exchanger, TcNHE1, has 11 transmembrane domains and is localized in acidic vacuoles of epimastigotes. The analyzed biochemical changes were correlated with morphological changes, including an increase in the size of acidocalcisomes and subsequent differentiation to an intermediate form. Both processes were delayed when TcNHE1 was inhibited by EIPA, suggesting that these early biochemical events allow the parasite to adapt to conditions faced in the rectum of the insect vector.

69   **1. Introduction**

70

71   The flagellate protozoan *Trypanosoma cruzi* is responsible for Chagas' disease, a

72   serious endemic illness prevalent throughout Latin America. This parasite has a

73   complex life cycle involving several morphological and functionally different stages

74   that adapt to a variety of conditions imposed by the insect vector and mammalian host

75   environments. The ability of *T. cruzi* to receive signals from different environments and

76   to initiate appropriate changes in cell activity is crucial for its pathogenic activity.

77   Previous evidences demonstrated that the parasite is able to respond to different

78   agonists by activation of a phosphatidylinositol 4,5 bisphosphate specific phospholipase

79   C (PI-PLC) [1,2], and consequently the inositol phosphate pathway [3,4]. *T. cruzi* PI-

80   PLC showed an absolute dependence on Ca^{2+} for its activity [5,6]. This enzyme contains

81   amino acid residues important for binding of InsP_3 and Ca^{2+} in the active site, as well as

82   putative Ca^{2+} ligands in the C2 domain. It is known that calcium signalling is required at

83   several points in the life cycle of *T. cruzi*, including host cell invasion [7],

84   multiplication, and differentiation [8].

85   Most of the releasable Ca^{2+} in trypanosomatids and apicomplexan parasites is

86   contained in acidocalcisomes which are acidic vacuoles that possess a Ca^{2+}/nH^+

87   exchanger, and several pumps [9]. In situations in which cells are exposed to NaCl

88   stress, the yeasts and plants have developed several mechanisms to maintain low levels

89   of salt in the cytoplasm, including removal of sodium by transport out of cell and/or into

90   the vacuoles by Na^+/H^+ exchanger activation [10]. *T. cruzi* acidocalcisomes share

91   several properties with vacuoles of plants, and a potential osmoregulatory function of

92   these acidic organelles [11]. In previous work [12], we showed dependence between

93   extracellular Na^+ and Ca^{2+} release from intracellular store evoked by Carbachol. In this

94   context, the slow component of Ca^{2+} signaling induced by the agonist was reduced in a

95   Na^+-free medium and progressively increased when the extracellular pH raised,

96   indicating that Ca^{2+} signaling was modified by a driving force imposed by opposite Na^+

97   and H^+ gradients. Thus, we suggested a model in which Na^+ and H^+ extracellular may

98   play an important regulatory role in allowing the phosphoinositide cycle to proceed in

99   the parasite response to certain extracellular signals. Moreover, Gimenez et al. [13]

100   demonstrated that high osmolarity during epimastigote growth leads to intermediate

101   forms, which showed PI-PLC activity higher than that of epimastigotes. These parasite

102   forms, considered to be a pre-adaptation of epimastigotes for differentiation to

103 tripomastigotes [14], were also found in the alimentary tract of reduviid insect where

104 epimastigotes propagate [15,16]. The environmental pH and Na^+ concentration vary

105 considerably in the triatomine gut and as a result, the osmolarity increases sharply to

106 600-1000 mOsm/l. However, an important question remaining is how the increased

107 osmolarity is transmitted into the parasite. Therefore, we studied the relationship

108 between increased osmolarity of the medium and phosphatidylinositol pathway in

109 epimastigotes of *T. cruzi,* mimicking the situation that the parasites encounter in the

110 insect's rectum where metacyclogenesis takes place. In this context, we found a Na^+/H^+

111 exchanger involvement in the PLC activation process, via stimulation by protein kinase

112 C and cytosolic calcium increase. Furthermore, we also show analysis of the amino acid

113 sequence, phylogenetic position and strong evidence that Na^+/H^+ exchanger is localized

114 in acidic vacuoles of *T. cruzi* epimastigotes.

115

116 **2. Materials and methods**

117

118 *2.1. Cells and culture media*

119 　　　The *Trypanosoma cruzi* Tulahuen strain was used in this study. Epimastigote

120 forms were grown at 28 ºC in culture medium supplemented with 10% fetal bovine

121 serum (FBS), as described previously by Machado de Domenech [1]. Cells in the

122 logarithmic phase of growth were harvested by centrifugation at 1500 g for 10 min and

123 washed twice with 25 mM Tris-HCl, pH 7.35, 1.2 mM $MgSO_4$, 2.6 mM $CaCl_2$, 4.8 mM

124 KCl, 120 mM NaCl, and 100 mM glucose [Krebs-Ringer-Tris (KRT) buffer].

125

126 *2.2. Measurement of alkalinization in acidic vesicles and epifluorescence microscopy*

127 　　　The alkalinization of vesicles in intact epimastigotes was assayed by measuring

128 changes in absorbance of Acridine Orange (AO) [17] using a GenesisTM

129 spectrophotometer (Spectronic®, Milton Roy Company) at the wavelength pair 493–

130 530 nm, described by Bollo et al. [12] and a spectrofluorometer Fluoromax 3 at

131 excitation and emission wavelength of 493 and 530 nm, respectively.

132 　　　Briefly, cells harvested in the logarithmic phase were suspended in 1.5 ml of

133 KRT buffer (5 x 10^7cells/ml), incubated with 10 μM AO for 30 s o 15 min, and added

134 with various effectors at 28 °C. In all cases, cells were preincubated with 1 μM 5-(N-

135 ethyl-N-isopropyl)-amiloride (EIPA) for 10 min prior to the addition of effectors. For

136   experiments under Na^+-free conditions, NaCl was replaced by 120 mM N-methyl-D-
137   glucamine (NMG).

138   For epifluorescence microscopy experiments, parasites were resuspended in
139   KRT buffer plus AO (10 μM) for 15 min at 28 °C, and washed twice in KRT buffer to
140   eliminate excess of dye. Parasites were then treated with various effectors for 15 min at
141   28 °C, and 10 μl aliquots were placed on the coverslips and observed under
142   epifluorescence microscope (Zeiss AxioLab Standard Fluorescence Microscopy) fitted
143   with a filter set 09 (Zeiss), excitation 450-490 nm and emission 510 nm.

144

145   *2.3. Measurement of $[Ca^{2+}]_i$ with Fura 2-AM*

146   Epimastigotes were harvested and washed once in KRT buffer. $[Ca^{2+}]i$ was
147   determined as described previous [12]. Briefly, cells were resuspended in KRT buffer (2
148   x 10^8 cells/ml), incubated with 4 μM Fura 2-AM in the dark for 60 min at 28 °C in a
149   water bath with mild agitation, washed twice with ice-cold KRT buffer, incubated for
150   20 min at 28 °C with agitation, and kept in ice in the dark until use. For fluorescence
151   measurement, a 0.375 ml aliquot of Fura 2-loaded epimastigote suspension was diluted
152   into 1.5 ml KRT buffer (final concentration 5 x 10^7 cells/ml), and placed in polystyrene
153   cuvets. Fluorescence was recorded in a DM3000 spectrofluorimeter (SPEX Industries,
154   Edison, NJ, USA) equipped with a thermostated (28 °C) cuvet holder and a stirring
155   device. Excitation and emission wavelengths were 340 and 500 nm, respectively.

156   Normalized fluorescence values were determined as described [18]. Calcium
157   release in response to effectors was determined by integrating the total fluorescence
158   signal obtained [19]. This value shows the amount of calcium released, relative to the
159   area under the transient curve for control, defined as 100%.

160

161   *2.4. Measurements of acidification in the cytoplasm*

162   Cytoplasmic acidification in intact epimastigotes was determined by changes in
163   the fluorescence of 2′,7′-bis-(Carboxyethyl)-5(6′)-carboxyfluorescein (BCECF), a pH
164   indicator. The experiments were carried out in spectrofluorometer Fluoromax 3 with
165   excitation wavelengths of 440 nm and 500nm, and with emission wavelength of 530
166   nm.

167   Parasites were suspended in KRT buffer-glucose-sulfinpyrazone (glucose 1.8%
168   w/v -sulfinpyrazone 200 M) pH 7.2. The cells were stabilized for 20 min, then added 9

169   M BCECF and incubated in the dark at 28 °C for 60 min. For measurements, 5×10^7

170   cells/ml in a final volume of 1.5 ml were loaded into cuvettes thermostatically

171   controlled at 28 ºC and the different effectors were added. The cells were pre-incubated

172   with 1 μM EIPA for 10 min prior to addition of effectors.

173

174   *2.5. Confocal microscopy*

175   Epimastigotes were harvested and washed twice with KRT buffer. A 10 l

176   aliquot (4×10^6 cells/ml) were fixed with methanol at -20 °C for 6 min, washed with

177   PBS and incubated with PBS-albumin for 30 min at room temperature. Parasites were

178   then incubated with anti-Na$^+$/H$^+$ and anti-VH$^+$ PPase, dissolved in PBS 1% v/v for 90

179   min, washed three times with PBS for 5 min and then incubated for 60 min with

180   secondary antibodies anti-goat IgG FITC labeled and anti-rabbit IgG Rhodamine

181   labeled, both dissolved in PBS 1% v/v. The cells were observed by confocal microscopy

182   Nikon Eclipse C1si spectral excitation with Argon laser line 488 for FITC and He-Ne

183   laser 543 for Rhodamine respectively.

184

185   *2.6. Electron microscopy*

186   Parasites were pre-incubated and gently agitated in a shaking water-bath for 10

187   min at 28 °C, in KRT buffer plus 0.1% bovine serum albumin (BSA), treated with 0.5

188   M NaCl or 1 M mannitol, added with ice-cold KRT buffer, and centrifuged at 1000 x g

189   for 5 min. The pellet was fixed with 2% glutaraldehyde and 4% formaldehyde in 0.1 M

190   cacodylate buffer pH 7.2 (buffer A) for 1 hr. The pellet was washed twice with buffer

191   A, fixed with 1% osmium tetroxide in buffer A, washed twice with water, dehydrated

192   with increasing acetone concentrations (up to 100%), and embedded in epoxy resin

193   (Araldite) for 24 hr at 60 ºC. Thin sections were cut by automated precision

194   ultramicrotome and observed in a LEO 906 transmission electron microscope (Zeiss,

195   Oberkochen, Germany). Vesicle diameter was measured in a significant number of cells

196   (at least 100 for each condition).

197

198   *2.7. Determination of morphological changes*

199   Epimastigotes were suspended in sterile KRT buffer (5×10^7 cells/ml) and

200   stabilized at 28 ºC. Then, the different effectors, in sterile conditions were added. The

201   cells were incubated during 2 hrs at 28 ºC and centrifuged at 1000 *g* during 10 min. The

202 pellets were transferred to a medium of differentiation, modified Grace´s (Sigma) and

203 were incubated at 28 ºC during 15 days.

204   For morphological studies, aliquots were taken each 24 hrs and parasites were

205 fixed with absolute methanol, and stained with 10% (v/v) Giemsa. At least 100

206 organisms were counted per sample in a Zeiss AxioLab Standard Fluorescence

207 Microscope. After Giemsa staining, the parasites were assigned to one of three classes:

208 epimastigotes, trypomastigotes, and intermediate forms between them.

209

210 *2.8. Measurement of myo-[^{3}H]inositol phosphates*

211   Cells harvested in the logarithmic phase were pre-incubated and gently agitated

212 in a shaking water-bath for 12 hrs at 28 ºC in KRT buffer containing 0.1% BSA, 10%

213 FBS, 3 mM $MnCl_2$ and 4 μCi *myo*-[^{3}H]inositol per 25 mg cells. These labelled cells

214 were then incubated in a shaking bath for 15 min at 28 ºC in KRT buffer containing

215 0.1% BSA, 10% FBS, and 10 mM LiCl. NaCl or mannitol were added to the indicated

216 concentrations for 15 min. Cells were preincubated with 1 μM U73122 for 20 min, 50

217 μM BAPTA-AM for 60 min, or 1 μM EIPA for 10 min prior to addition of effectors.

218 [^{3}H]Ins*P*s was separated by anion-exchange chromatography on Dowex AG 1-X8 as

219 described previously by Garrido et al. [2]. Briefly, neutralized extracts were applied to

220 columns of formate form resin and free inositol was eluted with 10 ml of water;

221 glycerophosphoinositols with 10 ml of 5 mM sodium tetraborate/60 mM ammonium

222 formate; inositol phosphate (Ins*P*) with 10 ml of 100 mM formic acid/200 mM

223 ammonium formate; Ins*P*$_2$ with 10 ml of 100 mM formic acid/400 mM ammonium

224 formate; Ins*P*$_3$ with 10 ml of 100 mM formic acid/800 mM ammonium formate and

225 Ins*P*$_4$ with 10 ml of 100 mM formic acid/1.2 M ammonium formate. The radioactivity

226 of each fraction was determined by mixing 25–700 μl samples of the column eluates

227 with 2–4 ml of Ready Safe-Liquid Scintilation cocktail. The results are expressed as the

228 relation between Ins*P*$_3$ and Ins*P*s.

229

230 *2.9. Sequence alignment and phylogenetic analysis*

231   Sequence analysis was performed using tools provided by the National Center

232 for Biotechnology Information (www.ncbi.nlm.nih.gov) and ExPASy Molecular

233 Biology Server (http://us.expasy.org). The *T. cruzi* genome database at GeneDB

234 (http://www.genedb.org/genedb/tcruzi) was searched using Wu-Blast2. Sequence

235 identity and similarity percentages were analyzed using BLASTP

236 (http://www.ncbi.nlm.nih.gov/blast/index.html). Sequences were initially aligned using

237 ClustalW (http://www.ebi.ac.uk/clustalw/) [20] with BioEdit Sequence Alignment

238 Editor 4.8.8 [21], and the alignment was then visually refined.

239 Hydrophobicity plot of the putative antiporter and transmembrane segments

240 were determined using TMPred program

241 (http://www.ch.embnet.org/software/TMPRED_form.html) [22]. Conserved sites of

242 phosphorylation for protein kinase C ([ST]) - x - [RK]) were searched using NetPhosK

243 1.0 (http://www.cbs.dtu.dk/ services/NetPhosK/) [23].

244 Phylogenetic tree was performed using Phylyp 3.6 software [24]. PAM distances

245 were computed on 419 reliably aligned sites by using ProtDist program. Phylogenetic

246 analysis was performed using the neighbor-joining method with 1000 bootstraps with

247 SeqBoot and Consense programs [25]. Obtained trees were viewed using the TreeView

248 1.6.6 program.

249

250 *2.10. Statistical analyses*

251 Student's "t" test was performed using STATGRAPHICS Plus version 5.0

252 (Statisticalaphics Corporation, Manugistics, Inc.). For statistical analysis of the size of

253 acidocalcisomes, non-parametric Kruskall-Wallis test was performed.

254

255 **3. Results**

256

257 *3.1. The hyperosmotic stress induced the alkalinization of acidocalcisomes via a*

258 *Na^+/H^+ exchanger and consequent calcium release*

259 In order to study the involvement of Na^+/H^+ exchanger in calcium signaling the

260 parasites were subjected to hyperosmotic stress. We took advantage of Acridine Orange

261 (AO), a membrane permeable dye that become protonated and sequestered into acidic

262 organelles. The presence of 0.5 M NaCl induced release of dye from acidic vacuoles,

263 indicating alkalinization of this organelle examined through changes in absorbance of

264 AO (**Fig. 1A**). A significant decrease in magnitude of this effect ($34.4 \pm 5.2\%$, *p<0.05*)

265 was observed in parasites pre-incubated with EIPA, the inhibitor of Na^+/H^+ exchanger.

266 Besides, when parasites were incubated in Na^+ free-medium (Na^+ replaced by

267 impermeable NMG), the alkalinization induced by NaCl was also partially suppressed

268 ($24.5 \pm 3.8\%$, *p< 0.05*). NH_4Cl which is in equilibrium with NH_3, a permeable weak

269 base, was used as a positive control. Addition of 20 mM NH_4Cl induced alkalinization

270 of the vacuoles.

271 NaCl is able to generate an increase in osmolarity of the medium and/or a Na^+

272 gradient increasing the driving force imposed by the opposing H^+ and Na^+ gradients.

273 We performed experiments to distinguish between these two possibilities by replacing

274 NaCl with mannitol. Mannitol (0.5 M) induced a lower release of dye than did NaCl

275 (37.2 ± 11.6%, *p<0.05*) (**Fig. 1B**). The alkalinization provoked by mannitol

276 significantly decreased when parasites were pre-treated with EIPA, or in Na^+-free

277 medium (56.0 ± 5.3% and 47.5 ± 14.8%, respectively, *p<0.05*).

278 Accumulation of AO in acidocalcisomes of epimastigote forms was also

279 detected by fluorescence microscopy (**Fig. 1C**, *Control*). Leakage of fluorescence upon

280 treatment with NaCl or mannitol confirmed the alkalinization of these acidic

281 compartments (**Fig. 1C**, *NaCl* and *mannitol*). Pre-treatment of parasites with EIPA

282 partially inhibited the decrease in fluorescence caused by hyperosmolarity, showing a

283 correlation between alkalinization and EIPA sensitive Na^+/H^+ exchanger activity in

284 these organelles (**Fig. 1C**, *EIPA-NaCl* and *EIPA-mannitol*).

285 The hyperosomotic stress (mannitol 0.5 M) also induced Ca^{2+} release (**Fig. 1D**,

286 *control*, 100%), and pre-treatment of parasites with EIPA significantly decreased Ca^{2+}

287 signal (*+EIPA*, 33.6 ± 6.4%, *p<0.01*). Also, a clear reversion of mannitol-induced Ca^{2+}

288 release was produced by replacing external Na^+ with NMG (*-Na⁺*, 45.1 ± 10.1%,

289 *p<0.05*), indicating that suppression of the Na^+/H^+ exchanger activity either by removal

290 of extracellular Na^+ or EIPA treatment partially inhibit calcium release.

291

292 *3.2. Involvement of PKC in vacuolar alkalinization induced by hyperosmotic stress*

293 The activator of PKC, phorbol-12-myristate-13-acetate ester (PMA) was able to

294 produce alkalinization of acidic vacuoles and this effect was reverted by EIPA (**Fig.**

295 **2A**), suggesting that the alkalinization was due to Na^+/H^+ exchanger activity which is

296 regulated by PKC. Moreover, PMA significantly increased (45 ± 7.5%, n=3, p<0.05)

297 alkalinization induced by 0.5 M mannitol, defined as 100% (**Fig. 2B**). This

298 alkalinization significantly decreased 35 ± 16.9% (n=3 p<0.05) when the parasites were

299 pre-treated with EIPA, confirming results observed in **Fig. 1B**. There was no significant

300 difference between the signals of EIPA and EIPA+PMA, indicating that the effect of the

301 PMA could not reverse the effect of the EIPA. This result was in agreement with the

302 effect of 1μM de Chelerythrine, a specific inhibitor of the kinase, which produced an

303   attenuation of $25 \pm 7.3\%$ (n=3 p<0.05) (**Fig. 2C**). There was no significant difference

304   between the signals of Chelerythrine and Chelerythrine+PMA. Again, PMA did not

305   reverse Chelerythrine effect; similar results were obtained with H7, inhibitor of PKC

306   (data not shown).

307   Hyperosmotic stress also provoked cytoplasmatic acidification determined by

308   fluorescence changes of BCECF, pH indicator (**Fig. 2D**). This effect was increased

309   when the parasites were pre-treated with PMA ($60 \pm 17.3\%$, n= 3 p<0.05). In addition,

310   the pre-treatment of parasites with EIPA+PMA partially decreased acidification $30 \pm$

311   8.7% (n= 3 p< 0.05).

312   These results suggest the involvement of an intracellular EIPA sensitive Na^+/H^+

313   exchanger, regulated by PKC, in vacuolar alkalinization and cytoplasmatic acidification

314   processes induced by hyperosmotic stress.

315

316   *3.3.   Hyperosmotic stress induces phospholipase C activation via a Na^+/H^+*

317   *exchanger*

318   We investigated whether calcium release induced by hyperosmotic stress is able

319   to activate PLC since it was demonstrated *T. cruzi*-PLC shows an absolute dependence

320   on Ca^{2+}. Treatment with NaCl or mannitol significantly increased InsP_3 levels relative

321   to unstimulated control (defined as 100%), $414 \pm 39\%$ and $315 \pm 33\%$, respectively

322   (**Fig. 3**) and total inositol phosphates (data not shown). These effects were reversed by

323   U73122, an inhibitor of PLC. Pre-incubation of parasites with BAPTA-AM, an

324   intracellular Ca^{2+} chelator, also blocked the InsP_3 accumulation induced by NaCl or

325   mannitol (**Fig. 3**). These findings indicate that PLC is dependent on cytosolic calcium

326   increase in response to hyperosmotic stress, under our experimental conditions. To

327   determine whether PLC activation by Ca^{2+} is dependent on ion release from

328   acidocalcisome mediated by Na^+/H^+ exchanger, epimastigotes were pre-incubated with

329   EIPA prior to hyperosmotic stress. EIPA reduced InsP_3 accumulation in either NaCl or

330   mannitol treatment (**Fig. 3**), suggesting that PLC activation occurs after Na^+/H^+

331   exchanger activation.

332

333   *3.4. Hyperosmotic stress induces morphological changes via a Na^+/H^+ exchanger*

334   Many organisms increase vacuolar volume in response to an osmotic challenge,

335   as a consequence of accumulation of Na^+ (along with Cl^- and water). By conventional

336   electron microscopy, we observed a significant increase in the size of acidocalcisomes

337 in parasites treated with NaCl ($34 \pm 7.3\%$, n= 112, *p<0.01*) or mannitol ($28 \pm 7.9\%$,

338 n=107, *p<0.01*), relative to control treated with vehicle (100%, **Fig. 4**, *-EIPA*, *upper*

339 *panels*). This effect was partially reversed by EIPA (**Fig. 4** *+EIPA*, *lower panels*).

340   On the other hand, the parasites grown in medium of modified Warren were

341 subjected to the treatment with 0.5 M NaCl or 1 M mannitol during 2 hrs in presence or

342 absence of EIPA and later transferred to a medium of differentiation, Grace´s modified.

343 **Fig. 5** shows that the treatment with high osmolarity induced an increase of 80% in

344 intermediate forms between epi- and trypomastigote at 150 hrs. In contrast, the presence

345 of EIPA in the medium of stimulation diminished to 20% the intermediate forms to the

346 same evaluated times. Therefore, it is possible to infer that the osmotic stress trigger

347 signals that lead to morphological changes, indicative of the induction of the

348 metacyclogenesis. Together, our results suggested the involvement of a Na^+/H^+

349 exchanger of acidocalcisomes would be compromised in these early events that lead to

350 the differentiation process in *T. cruzi*.

351

352 *3.5. Analysis of the amino acid sequence of Na^+/H^+ exchanger in T. cruzi*

353   To provide additional support for the Na^+/H^+ exchanger involvement in *T. cruzi*

354 calcium signaling, we performed the sequence analysis of this antiporter in this parasite.

355 The parasite genome [26] contains an open reading frame of 3627 nucleotides which

356 codifies a putative Na^+/H^+ antiporter (Access number XP_808429.1) of 1208 amino

357 acid residues with a calculated molecular mass of 136 kDa. The deduced sequence is

358 composed of 42% of hydrophobic, 23% polar, 9% basic, and 10% acidic amino acids. A

359 hydropath plot generated with the program TMPRED indicated that the N-terminal

360 portion of this protein contains 11 putative hydrophobic regions and that C-terminal

361 portion is hydrophilic (**Fig. 6A, B**). These hydrophobic regions are probably membrane-

362 spanning segments, similar to the topologies predicted for other Na^+/H^+ exchangers.

363   Database searches revealed substantial similarities between the predicted

364 transmembrane region of XP_808429.1 and Na^+/H^+ antiporters of animal, vegetal and

365 microbial origins (**Table 1**). N-terminal portion of *T. cruzi* exchanger has 47%

366 similarity with the organellar Na^+/H^+ exchanger from *Toxoplasma gondii* and the

367 greatest similarity with putative Na^+/H^+ antiporter from *Leishmania major*, a parasite

368 closely related to *T. cruzi*. These findings demonstrate that the putative protein has the

369 same structural characteristics than Na^+/H^+ antiporters of diverse origins and suggest its

370 function as a Na^+/H^+ exchanger, therefore in this work XP_808429.1 will be called

371 TcNHE1 and its ORF, Tcnhe1, since it is the first Na^+/H^+ exchanger described in

372 *Trypanosome cruzi.*

373   In order to determine the family or subfamily of TcNHE1, a phylogenetic

374 analysis was performed using Na^+/H^+ exchanger protein sequences from different

375 organisms. The sequences were aligned using ClustalW program and the tree was

376 performed with the most conserved portion of these proteins (aa 18-437 in TcNHE1)

377 using PHYLYP program (**Fig. 7**). TcNHE1 clustered with NhaP/SOS1 exchangers

378 which include Na^+/H^+ exchangers from prokaryotes, plants, fungi and protozoa.

379

380 *3.6. Analysis of expression of Tcnhe1*

381   It is known that Na^+/H^+ exchangers are widely distributed in organisms across all

382 phyla and kingdoms. However, at the present, there are only biochemical evidences that

383 demonstrate the functionality of this protein in acidocalcisomes of *T. cruzi*

384 epimastigotes. To further investigate the possibility that Tcnhe1 is expressed in the

385 parasite, an analysis of RT-PCR was carried out. Total RNA was extracted from

386 epimastigotes and cDNA was obtained by reverse transcription. Tcnhe1 sequence was

387 amplified using gene-specific primers; **Fig. 8** shows the amplification of a band between

388 3 and 4 Kpb which correlates with the predicted size of Tcnhe1. PCR-amplified product

389 was extracted and sequenced. Alignments between the sequenced fragments and Tcnhe1

390 showed high identity (98%, supplementary data). This result demonstrates the presence

391 of *Tcnhe1* transcript in *T. cruzi* epimastigotes.

392

393 *3.7. Immunofluorescence localization of Na^+/H^+ exchanger in T. cruzi epimastigote*

394 *forms*

395   In order to corroborate the intracellular localization of Na^+/H^+ exchanger,

396 immunofluorescence analysis of permeabilized cells were carried out. An antibody

397 against vacuolar-H^+PPasa, acidocalcisome marker [27], was used for comparison. As

398 shown in **Fig. 9**, a strong co-localization of anti-Na^+/H^+ exchanger with vacuolar-

399 H^+PPasa in the acidocalcisome was detected. This demonstrated that TcNHE1 is

400 localized in acidic vacuoles.

401

402 **4. Discussion**

403

404   High osmolarity stress caused by NaCl has been widely studied in many cell

405 types. An important common biochemical event is the activity of Na^+/H^+ exchangers in

406 subcellular organelles [28]. This antiporter mechanism has been implicated in pH

407 homeostasis regulation, cell volume control, and adaptation to high salinity, averting the

408 damaging effects of Na^+ on key biochemical processes in the cytosol [29,30]. In *T.*

409 *cruzi,* a gradient of Na^+ between extracellular medium and organellar lumen favours

410 calcium release from acidic vacuoles via an EIPA-sensitive-Na^+/H^+ exchanger. The

411 acidic compartment alkalinization of the parasite induced by monensin-Na^+/H^+

412 ionophore and its effect on the calcium signal indicate a relationship between the

413 alkalinization process of the vacuoles and Ca^{2+} release. Moreover, the effect of

414 monensin on $[Ca^{2+}]_i$ was independent of extracellular calcium, indicating that the cation

415 is released from intracellular stores [12]. The acidic pH inside acidocalcisomes favours

416 Ca^{2+} retention, and, a prior pH gradient neutralization between organellar lumen and

417 cytosol is therefore necessary for effective Ca^{2+} release from these acidic vacuoles [31].

418 Here, we show the involvement of EIPA-sensitive Na^+/H^+ exchanger in response to

419 hyperosmolarity, determined by alkalinization of these acidic vacuoles. As EIPA is a

420 competitive inhibitor [32], when high Na^+ concentrations were utilized, it was not

421 possible to obtain total inhibition of the alkalinization. This concept is supported by the

422 fact that more effective EIPA inhibition was observed either with mannitol or under Na^+

423 absence condition (Fig. 1A, B). High osmolarity treatment led to calcium release as a

424 consequence of Na^+/H^+ exchanger activation, since absence of extracellular Na^+ or

425 presence of EIPA partially inhibited the calcium increase. Taken together, these results

426 indicate a mechanism of parasite adaptation to high osmolarity, similar to the situation

427 faced by epimastigotes in the rectum of the insect vector.

428   It's well known that in several cell types, PKC may activate Na^+/H^+ exchanger

429 and it mediates the response to a multitude of regulatory signals involved in the control

430 of cell proliferation, differentiation and osmolarity changes [29,33]. Here, we showed

431 the activity of a PKC regulated-Na^+/H^+ exchanger in *T. cruzi*, since the vacuolar

432 alkalinization was induced by PMA and reversed both by EIPA and chelerythrine.

433 Moreover, the *in silico* analysis of the antiporter of *T. cruzi* (TcNHE1) revealed several

434 PKC phosphorylation sites ([ST]) - x - [RK]) located in the C-terminal region. Our

435 results are in agreement with the fact that Wainszelbaum et al. [34] observed the

436 presence of a band of molecular mass similar to those predict for TcNHE1, when they

437 analyzed the phosphorylation pattern of PMA-treated epimastigotes. Thus, our results

438   suggest that *T. cruzi* Na^+/H^+ exchanger is phosphorylated by PKC as occur in the higher

439   eukaryotes [35,36] and such mechanism would participate in the regulation of the

440   cytoplasmatic pH in response to hyperosmotic stress. This response could be similar to

441   the evoked by Carbachol, which induces alkalinization of acidic vacuoles and calcium

442   release via Na^+/H^+ exchanger activation and subsequent activation of a Ca^{2+}/nH^+

443   exchanger [12]. Indeed, a strong co-localization of TcNHE1 with a vacuolar-type

444   H^+PPasa, acidocalcisome marker [27], was detected. The *in silico* analysis of TcNHE1

445   showed that this protein is homologous to Na^+/H^+ exchangers of plants, fungi, protozoa,

446   bacteria and animals. The phylogenetic analysis revealed that this antiporter belongs to

447   the NhaP/SOS1 family, therefore could be located both in intracellular and plasma

448   membrane as occurs in *Toxoplasma gondii* [30]. Our results demonstrate that TcNHE1

449   is located, at least in part, in acidic vacuoles of *T. cruzi*.

450   The inhibition of Na^+/H^+ exchanger by EIPA, which affected calcium release

451   from acidocalcisome, also suppressed the InsP_3 level associated with high osmolarity,

452   suggesting the idea that PLC activation is a consequence of Ca^{2+} release from

453   acidocalcisome. Indeed, chelation of intracellular calcium suppressed the InsP_3 increase

454   induced by hyperosmotic stress and the Ca^{2+} release was reversed by U73122, a PLC

455   inhibitor. In agreement with this, Nozaki et al. [5] and Furuya et al. [6] demonstrated an

456   absolute dependence on Ca^{2+} for PLC activity in *T. cruzi*. Our previous [13] and present

457   results show that phospholipase C is clearly involved in the response to hyperosmotic

458   stress in epimastigote forms of *T. cruzi*.

459   The compartmentation of Na^+ into vacuoles allows the organism to use NaCl as

460   an osmoticum, maintaining an osmotic potential that drives water into cells. Thus, the

461   increase of the size of epimastigote acidic vacuoles, when cells are exposed to NaCl,

462   allows the adaptation of parasites to hyperosmotic stress. Similar results were observed

463   by Blumwald et al. [10] in plant cell. The accumulation of Na^+ by Na^+/H^+ exchanger in

464   the organellar lumen may cause uptake of water and consequent swelling of the vacuole,

465   which has been involved in osmoregulation of free living and parasite protists [37]. This

466   idea is supported by the partial reversion of acidocalcisome swelling observed in EIPA-

467   treated parasites.

468   Development of *T. cruzi* in the reduviid insect vector is an important step for the

469   transmission of the protozoan. Traditionally, two forms of the parasite are described in

470   the vector: epimastigotes and metacyclic trypomastigotes. However, intermediate forms

471   between epi- and tripomastigotes, which are characterized by flagellar elongation, have

472 also been reported by Kollien and Schaub [38], suggesting a process of continuous
473 transformation among stages. We show here that an increase of osmolarity of the
474 medium to ~600-1000 mOsm/l, caused by NaCl or mannitol addition, induces
475 development of these intermediate forms. The exposition of the epimastigotes to a
476 medium hyperosmolar would be a process that conduce to differentiation and would
477 allow to the parasites to survive to an environment of high salinity. Thus, Carvalho-
478 Moreira et al. [39] showed that epimastigotes incubated in saline solution begin
479 metacyclogenesis, but failed to complete the process, that is interrupted in the
480 intermediate stage. Moreover, in a previous work we demonstrated that high osmolarity
481 during epimastigote growth leads to intermediate forms [13], which were also increased
482 in parasites maintained in glucose-free medium [14], or when *in vitro* diuresis was
483 induced by artificial diuretic hormone 5-hydroxytryptamine (5-HT) in isolate whole
484 recta of *T. infestans* [15,38]. A delay in the apparition of the intermediate forms due to
485 the stimulation of the parasites in a short period of 2 hrs in presence of EIPA was
486 observed, suggesting the participation of Na^+/H^+ exchanger in the process of
487 differentiation. Therefore, the activation of the different pathways previously mentioned
488 in response to the high osmolaridad might be involved in the biochemical events that
489 lead to the differentiation.

490   In summary, our results show that hyperosmolarity induces PLC activation
491 mediated by Ca^{2+} release from acidocalcisome, which is favoured by alkalinization of
492 the vacuole via a Na^+/H^+ exchanger. We suggest that these early biochemical events
493 allow the parasite to adapt to conditions faced in the rectum of the insect vector, and
494 could be key steps in the differentiation process.

495

496 **5. Acknowledgments**

497

505

6. References

[1] E. Machado de Domenech, M. Garcia, M. Garrido, G. Racagni, Phospholipids of *Trypanosoma cruzi*: increase of polyphosphoinositides and phosphatidic acid after cholinergic stimulation, FEMS Microbiol. Lett. 74 (1992) 267-270.

[2] M. Garrido, M. Bollo, E. Machado-Domenech, Biphasic and dose-dependent accumulation of INSP$_3$ in *Trypanosoma cruzi* stimulated by a synthetic peptide carrying a chicken alpha D-globin fragment, Cell Mol. Biol. 42 (1996) 859-864.

[3] N. Marchesini, M. Bollo, G. Hernández, M. Garrido, E. Machado-Domenech, Cellular signalling in *Trypanosoma cruzi*: biphasic behaviour of inositol phosphate cycle components evoked by carbachol, Mol. Biochem. Parasitol. 120 (2002) 83-91.

[4] V. Santander, M. Bollo, E. Machado-Domenech, Lipid kinases and Ca^{2+} signaling in *Trypanosoma cruzi* stimulated by a synthetic peptide, Biochem. Biophys. Res. Commun. 293 (2002) 314-320.

[5] T. Nozaki, A. Toh-e, M. Fujii, H. Yagisawa, M. Nakazawa, T. Takeuchi, Cloning and characterization of a gene encoding phosphatidyl inositol-specific phospholipase C from *Trypanosoma cruzi*, *Mol. Biochem. Parasito.l* 102 (1999) 283-295.

[6] T. Furuya, C. Kashuba, R. Docampo, S. Moreno, A novel phosphatidyl inositolphospholipase C of *Trypanosoma cruzi* that is lipid modified and activated during trypomastigote to amastigote differentiation, J. Biol. Chem. 275 (2000) 6428-6438.

[7] M. Yakubu, S. Majumder, F. Kierszenbaum, Changes in *Trypanosoma cruzi* infectivity by treatments that affect calcium ion, Mol. Biochem. Parasitol. 66 (1994) 119-125.

[8] E. Lammel, M. Barbieri, S. Wilkowsky, F. Bertini, E. Isola, *Trypanosoma cruzi*: involvement of intracellular calcium in multiplication and differentiation, Exp. Parasitol. 83 (1996) 240-249.

[9] R. Docampo, S.N.J. Moreno, The acidocalcisome, Mol. Biochem. Parasitol. 114 (2001) 151-159.

[10] E. Blumwald, G. Aharon, M. Apse, Sodium transport in plant cells, Biochim. Biophys. Acta. 1465 (2000) 140-151.

[11] A. Montalvetti, P. Rohloff, R. Docampo, A functional aquaporin co-localizes with the vacuolar proton pyrophosphatase to acidocalcisomes and the contractile vacuole complex of *Trypanosoma cruzi,* J. Biol. Chem. 279 (2004) 38673-38682.

540   [12] M. Bollo, S. Bonansea, E. Machado, Involvement of Na$^+$/H$^+$ exchanger in the

541   calcium signaling in epimastigotes of *Trypanosoma cruzi*, FEBS Lett. 580 (2006) 2686–

542   2690.

543   [13] A.M. Gimenez, V.S. Santander, A.L. Villasuso, S.J. Pasquaré, N.M. Giusto, E.E.

544   Machado, Regulation of Phosphatidic Acid Levels in *Trypanosoma cruzi,* Lipids 46

545   (2011) 969-979.

546   [14] K. Tyler, D. Engman, Flagellar elongation induced by glucose limitation is

547   preadaptive for *Trypanosoma cruzi* differentiation, Cell. Motil. Cytoskeleton 46 (2000)

548   269-278.

549   [15] A. Kollien, G. Schaub, *Trypanosoma cruzi* in the rectum of the bug Triatoma

550   infestans: effects of blood ingestion of the vector and artificial dieresis, Parasitol. Res.

551   83 (1997) 781-788.

552   [16] A. Kollien, G. Schaub, Ionic composition of the rectal contents and excreta of the

553   reduviid bug Triatoma infestans, J. Insect. Physiol. 47 (2001) 739-747.

554   [17] M. Palmgren, Acridine orange as a probe for measuring pH gradients across

555   membranes: mechanism and limitations, Anal. Biochem. 192 (1991) 316-321.

556   [18] A. Takahashi, P. Camacho, J. Lechleiter, B. Herman, Measurement of intracellular

557   calcium, Physiol. Rev. 79 (1999) 1089-1125.

558   [19] M. Bollo, G. Venera, M. Biscoglio de Jimenez Bonino, E. Machado-Domenech,

559   Binding of nicotinic ligands to and nicotine-induced calcium signaling in *Trypanosoma*

560   *cruzi*, Biochem. Biophy. Re. Commun. 281 (2001) 300-304.

561   [20] J.D. Thompson, D.G. Higgins, T.J. Gibson, CLUSTAL W: improving the

562   sensitivity of progressive multiple sequence alignment through sequence weighting,

563   position-specific gap penalties and weight matrix choice, Nucleic Acids Res. 22 (1994)

564   4673–4680.

565   [21] T.A. Hall, BioEdit: a user-friendly biological sequence alignment editor and

566   analysis program for Windows 95/98/NT, Nucl. Acids Symp. Ser. 41 (1999) 95–98.

567   [22] K. Hofmann, W. Stoffel, TMbase - A database of membrane spanning proteins

568   segments, Biol. Chem. Hoppe-Seyler 374 (1993) 166.

569   [23] N. Blom, T. Sicheritz-Ponten, R. Gupta, S. Gammeltoft, S. Brunak, Prediction of

570   post-translational glycosylation and phosphorylation of proteins from the amino acid

571   sequence, Proteomics 4,6 (2004) 1633-1649.

572   [24] J. Felsenstein, Phylogenies from Molecular Sequences: Inference and Reliability

573   Annual Review of Genetics, 22 (1988) 521-565.

574   [25] N. Saitou, M. Nei, The neighbor-joining method: a new method for reconstructing

575   phylogenetic trees, Mol. Biol. Evol. 4 (1997) 406–425.

576   [26] N.M. El-Sayed, P.J. Myler, D.C. Bartholomeu, D. Nilsson, G. Aggarwal, A.N.

577   Tran et al, The genome sequence of *Trypanosoma cruzi*, etiologic agent of Chagas

578   disease, Science 309 (2005) 409-415.

579   [27] D.A. Scott, W. de Souza, M. Benchimol, L. Zhong, H.G. Lu, S.N. Moreno, R.

580   Docampo, Presence of a plant-like proton-pumping pyrophosphatase in acidocalcisomes

581   of *Trypanosoma cruzi*, J. Biol. Chem. 273 (1998) 22151-22158.

582   [28] E. Padan, S. Schuldiner, Molecular physiology of Na^+/H^+ antiporters, key

583   transporters in circulation of Na^+ and H^+ in cells, Biochim. Biophys. Acta. 1185 (1994)

584   129-151.

585   [29] R. Nass, R. Rao, Novel localization of a Na^+/H^+ exchanger in a late endosomal

586   compartment of yeast, Implications for vacuole biogenesis, J. Biol. Chem. 273 (1998)

587   21054-21060.

588   [30] M. Francia, S. Wicher, D. Pace, J. Sullivan, S. Moreno, G. Arrizabalaga, A

589   *Toxoplasma gondii* protein with homology to intracellular type Na^+/H^+ exchangers is

590   important for osmoregulation and invasion, Exp. Cell Res. 317 (2011) 1382-1396.

591   [31] A.E. Vercesi, R. Docampo, Sodium-proton exchange stimulates Ca^{2+} release from

592   acidocalcisomes of *Trypanosoma brucei*, Biochem. J. 315 (1996) 265-270.

593   [32] T.R. Kelyman, E.J. Cragoe jr, Amiloride and its analogs as tools in the study of ion

594   transport, J. Membr. Biol. 105 (1988) 1-21.

595   [33] H. Wang, D. Singh, L.J. Fliegel, The Na^+/H^+ antiporter potentiates growth and

596   retinoic acid-induced differentiation of P19 embryonal carcinoma cells, J. Biol. Chem.

597   272 (1997) 26545-26549.

598   [34] M.J. Wainszelbaum, M.L. Belaunzarán, E.M. Lammel, M. Florin-Christensen, J.

599   Florin-Christensen, E.L.D. Isola, Free fatty acids induce cell differentiation to infective

600   forms in *Trypanosoma cruzi*, Biochem. J. 375 (2003) 705–712.

601   [35] S. Busch, T. Wieland, H. Esche, K.H. Jakobs, W. Siffert, G protein regulation of

602   the Na^+/H^+ antiporter in Xenopus laevis oocytes. Involvement of protein kinases A and

603   C, J. Biol. Chem. 270 (1995) 17898-17901.

604   [36] S.F. Pederson, C. Varming, S.T. Christensen, E.K. Hoffmann, Mechanisms of

605   activation of NHE by cell shrinkage and by calyculin A in Ehrlich ascites tumor cells, J.

606   Membr. Biol. 189 (2002) 67-81.

607   [37] R. Docampo, P. Ulrich, S.N.J. Moreno, Evolution of acidocalcisomes and their role

608   in polyphosphate storage and osmoregulation in eukaryotic microbes, Phil. Trans. R.

609   Soc. B. 365 (2010) 775-784.

610   [38] A. Kollien, G. Schaub, The development of *Trypanosoma cruzi* in Triatomine,

611   Parasitol. Today 16 (2000) 381-387.

612   [39] C.J. Carvalho-Moreira, M.C.D. Spata, J.R. Coura, E.S. Garcia, P. Azambuja, M.S.

613   Gonzalez, C.B. Melloc, In vivo and in vitro metacyclogenesis tests of two strains of

614   *Trypanosoma cruzi* in the triatomine vectors Triatoma pseudomaculata and Rhodnius

615   neglectus: short/long-term and comparative study, Exp. Parasitol. 103 (2003) 102-11.

616

617   **Figure captions:**

618

619   **Figure 1. Effect of hyperosmotic stress on acidocalcisome alkalinization and**

620   **calcium release.** Epimastigotes were resuspended to a final density of 5 x 10^7 cells/ml

621   in KRT buffer (*control*), in KRT buffer without Na^+ (*-Na*$^+$), or in the presence of 1 μM

622   EIPA for 10 min prior to treatment (+*EIPA*). AO: 10 μM acridine orange. 20 mM

623   *NH$_4$Cl*. Arrows indicate addition of 0.5 M NaCl (*A*) or mannitol (*B*). A representative

624   experiment is shown (*n=5*, each performed in triplicate). *C*) Cells were resuspended in

625   KRT buffer plus 10 μM Acridine Orange and incubated for 15 min at 28 °C in a water

626   bath with mild agitation. Parasites were treated with vehicle (*control*) or 0.5 M NaCl or

627   mannitol with or without 1 μM EIPA for 10 min prior to treatment. Arrows indicate

628   accumulated dye inside the acidic compartment. A representative photograph is shown

629   (*n=3*). Scale bar = 10 μm. *D*) Epimastigotes loaded with Fura-2 were resuspended in

630   KRT buffer (*control*), in KRT buffer without Na+ (*-Na*$^+$), or in the presence of 1 μM

631   EIPA for 10 min prior to treatment (+*EIPA*). Arrows indicate addition of 0.5 M

632   mannitol. A representative experiment is shown (*n* = 6, each performed in triplicate).

633

634   **Figure 2. Role of PKC in vacuolar alkalinization evoked by hyperosmotic stress.**

635   Parasites (5 × 10^7 cells/ml) were harvested, washed with KRT/glucose- sulphinpyrazone

636   and loaded with AO 15 min *(A, B and C)* or with BCECF *(D)*. PKC activator (1 μM

637   PMA) under basal conditions (*A*) and conditions of hyperosmotic stress, mannitol 0.5 M

638   *(B and C)* or mannitol 0.75 M *(D)*, was used both in the presence or absence of EIPA.

639   PKC inhibitor Chelerythrine 1 μM was used *(C)*. A representative experiment is shown

640   (*n= 3*, each performed by duplicate).

641

Figure 3. Accumulation of InsP_3 in epimastigotes in response to hyperosmotic stress. Epimastigotes labeled with *myo*-[^{3}H]inositol and resuspended in KRT buffer were pre-incubated with inhibitors and treated with 0.5 M NaCl or mannitol. *U73122,* 1x10^{-5} M for 10 min. *BAPTA-AM,* 5x10-5 M for 60 min. *EIPA,* 1 μM for 10 min. Results are expressed as percent of non stimulated control (defined as 100%). Values are mean ± S.E (*n=5*).

648 **Figure 4. Effect of hyperosmotic stress on size of acidocalcisomes.** Epimastigotes were fixed and observed directly by electron microscopy as described in M&M. Cells were treated with vehicle (control), 0.5 M NaCl, or mannitol, in the absence or presence of 1 μM EIPA for 10 min. Arrows indicate the acidic compartment. Scale bar = 1.5 μm. *Inset*, amplification of region showing a set of acidocalcisomes.

653 **Figure 5. Effect of EIPA on morphologic changes induced by hyperosmotic stress.** Epimastigotes were harvested and washed with KRT buffer in sterile conditions. Parasites were subjected to hyperosmotic stress through addition of 0.5 M NaCl (A) or 1M mannitol (B), transferred to modified Grace's medium and grown during 13 days. 1 μM EIPA was added before treatments when is indicated. Samples were taken each 24 h and percentages of intermediate forms were calculated. Results are expressed as percent of total parasites (defined as 100%). Values are mean ± S.E (*n=2*).

660

661 **Figure 6. Analysis of TcNHE1 amino acidic sequence.** Deduced amino acidic sequence of the putative antiporter TcNHE1 (A). The 11 putative transmembrane domains (TM) are indicated with *black bars*. Predicted PKC phosphorylation sites are shown in *open boxes*. Hydrophobicity plot of TcNHE1 was calculated by the programme TMPRED (B). Portions above and below the midpoint line indicate hydrophobic and hydrophilic regions respectively. Eleven putative transmembrane domains are shown.
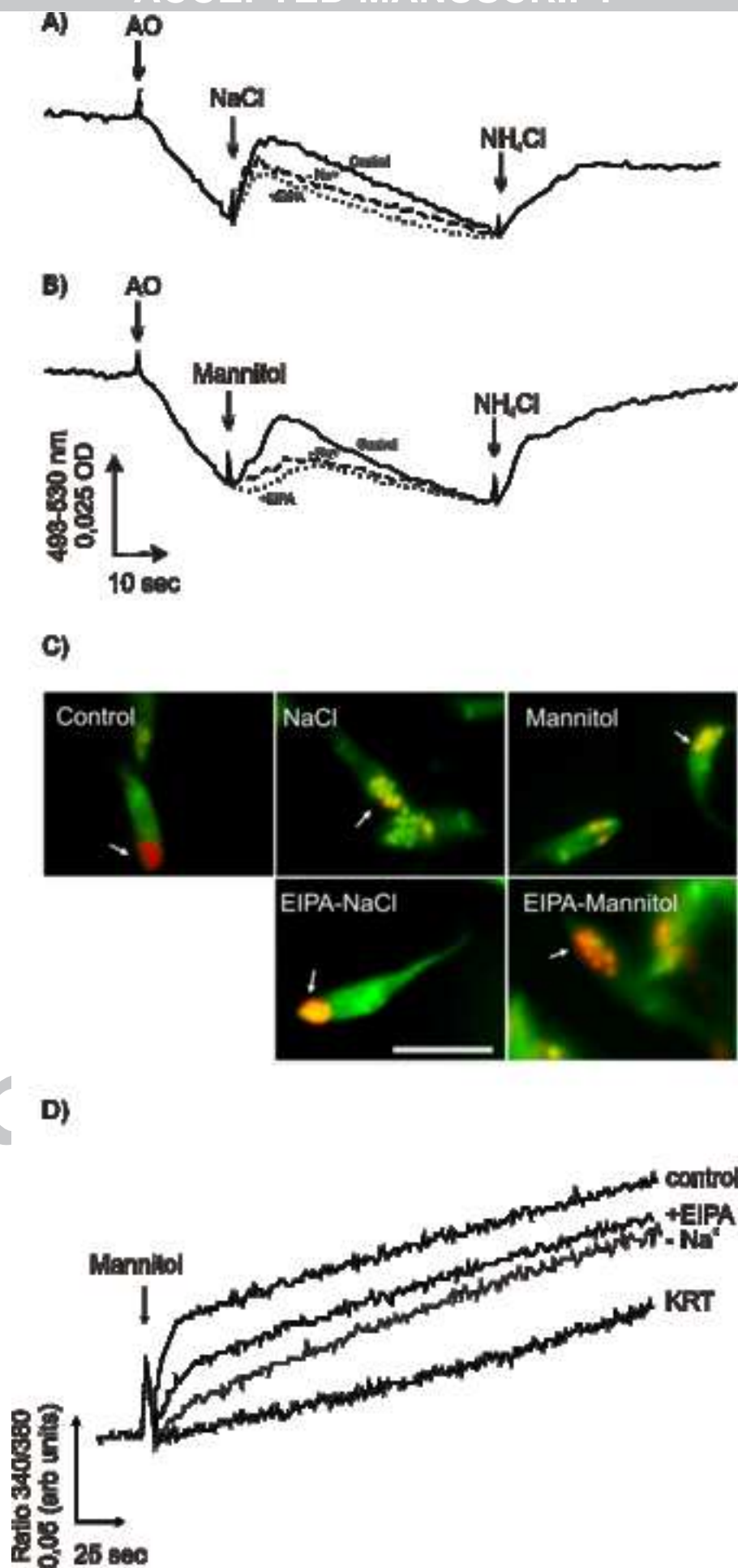
668

669 **Figure 7. Phylogenetic analysis between Na$^+$/H$^+$ exchangers based on amino acid sequence comparison.** The phylogenetic analysis was carried out using PHYLIP 3.6. The accessions numbers and sources of each of the other representatives Na$^+$/H$^+$ antiporters are: NHE1 (NP_003038.2), NHE2 (NP_003039.2); NHE3 (NP_004165.1),
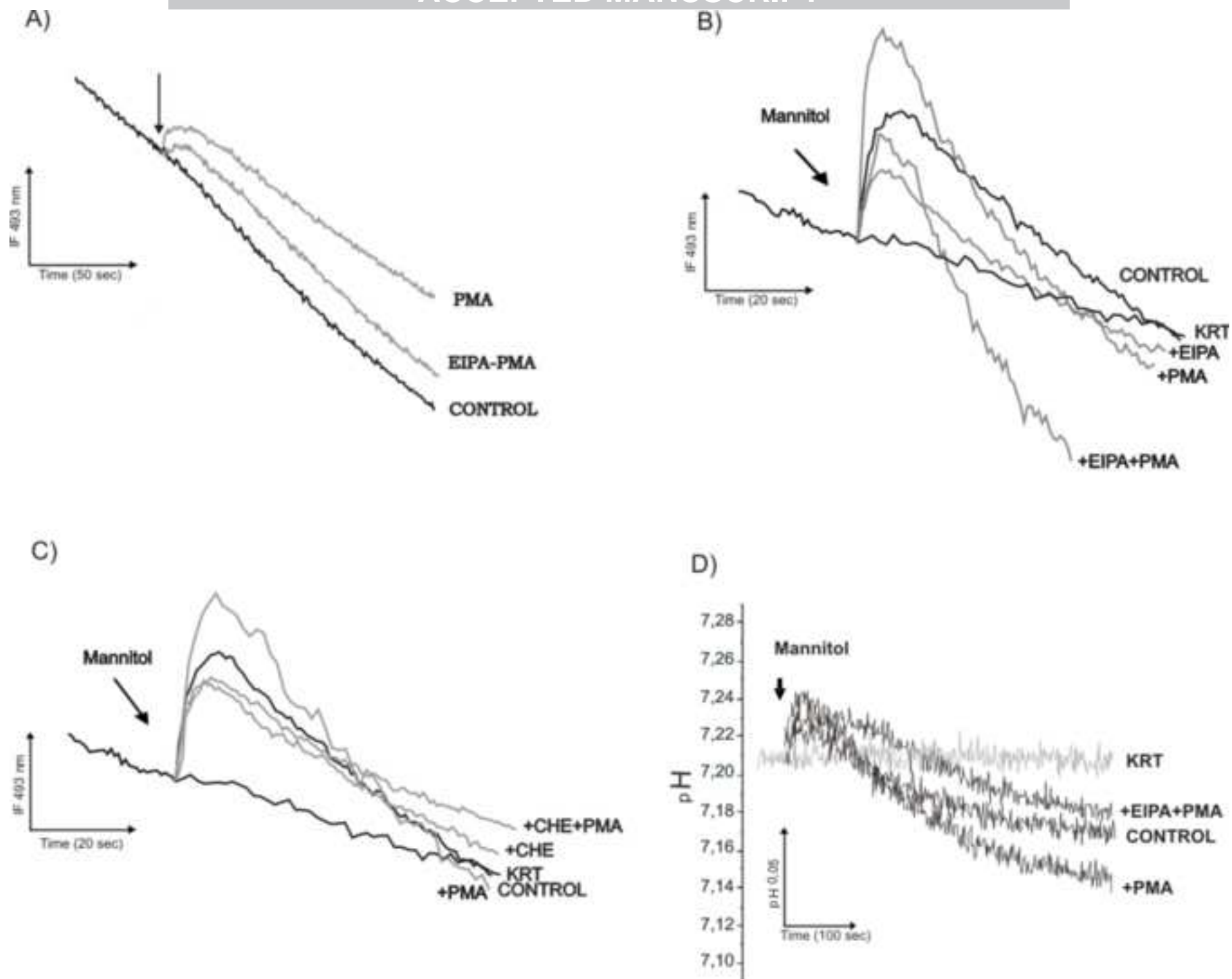
673   NHE4 (XP_351480.1), NHE5 (NP_004585.1), NHE6 (NP_006350.1), NHE7

674   (NP_115980.1), NHE8 (NP_05608.1) and NHE9 (NP_775924.1) from *Homo sapiens;*

675   NHX1 (NP_198067.1), NHX2 (NP_187154), NHX8 (AAZ76246.1) and SOS1

676   (NP_178307.2) from *Arabidopsis thaliana*; NHX1 (AAQ63678.1) and SOS1

677   (AAP93587.1) from *Oryza sativa*; SOS1 (CAD203220.1) *Cymodocea nodosa*; SOS1

678   (CAD911921.1) *Physcomitrella patens*; NHX1 (NP_010744.1) *Saccharomyces*

679   *cerevisiae*; (AAO52201.1) *Dictyostelium discoideum*; (CAJ04461.1) *Leishmania major*;

680   SOS1 (CAD98616.1) *Cryptosporidium parvum*; NHE1 (AAR85890.1) and NHE2

681   (AAU81711.1) from *Toxoplasma gondii;* SOS1 (CAH93661.1) *Plasmodium berghei*;

682   SOS1 (EAA22449.1) *Plasmodium yoelii yoelii*; SOS1 (XP_745140.1) *Plasmodium*

683   *chabaudi* and SOS1 (NP_704934.1) *Pasmodium falciparum.*
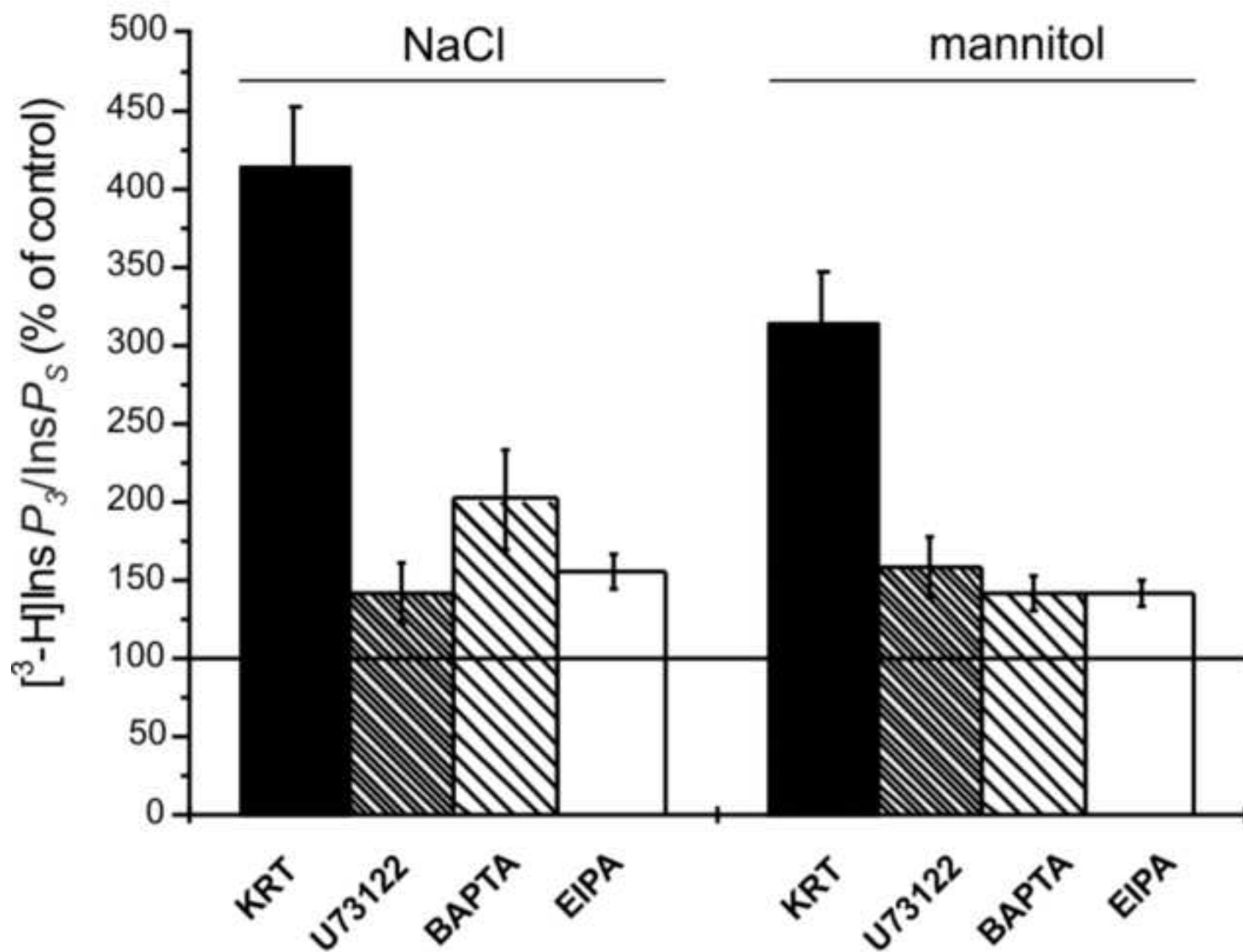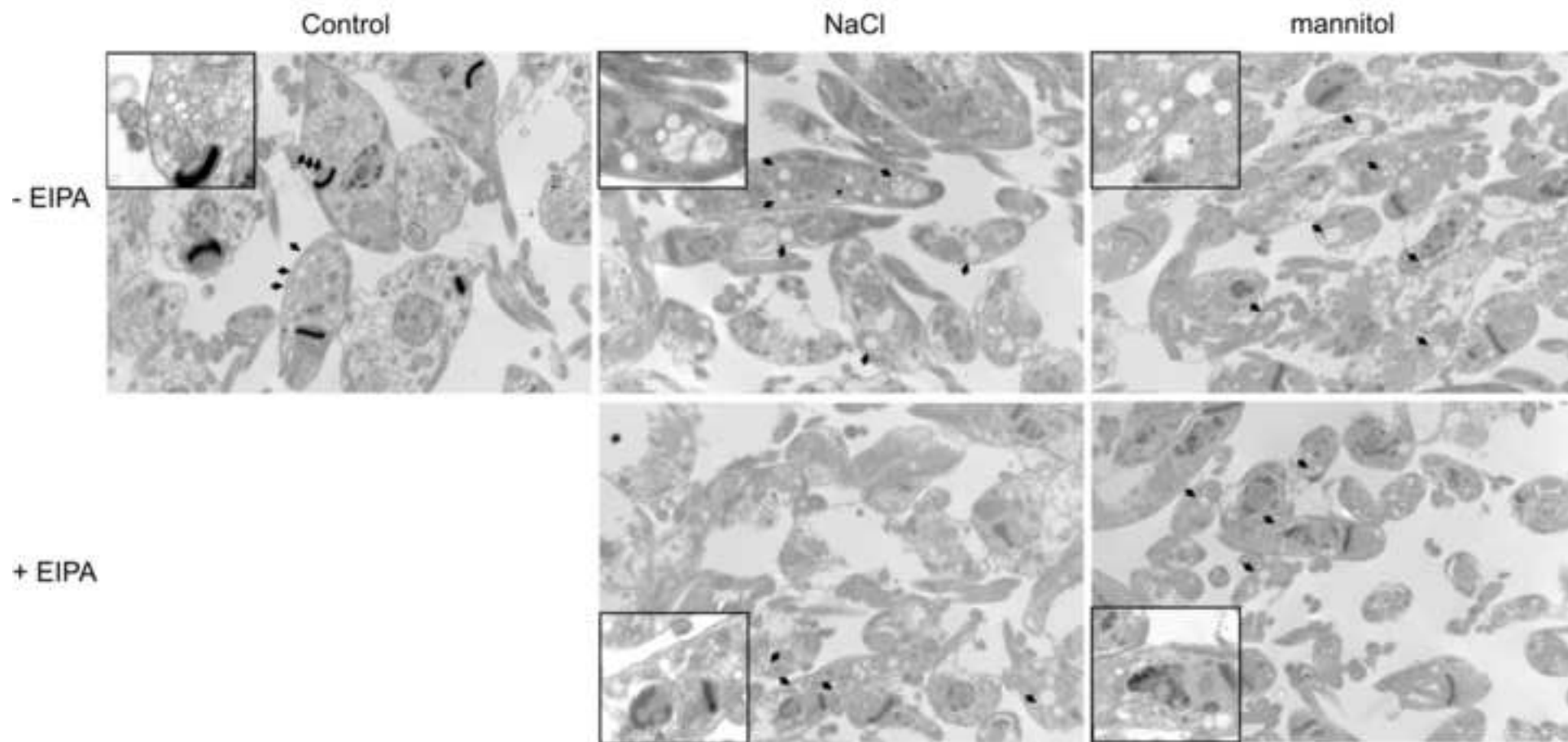
684

685   **Figure 8. Expression of Na$^+$/H$^+$ exchanger in *T. cruzi* epimastigote forms**. Purified

686   RNA from epimastigotes of *T. cruzi* was used for RT-PCR analysis to amplify Tcnhe1.

687   The resulting PCR products were separated on an agarose gel. (1) Molecular size

688   markers (pairbases). (2) PRC products. 3) Negative control.

689   **Figure 9. Localization of Na$^+$/H$^+$ exchanger in epimastigotes of *T. cruzi*.** Parasites

690   were fixed and incubated with primary antibodies anti-Na$^+$/H$^+$ and anti-VH$^+$ PPase.

691   Secondary antibodies anti-goat IgG FITC labeled and anti-rabbit IgG Rhodamine

692   labeled were used. Cells were observed by confocal microscopy Nikon Eclipse C1si

693   spectral excitation in bright-field (A), with Argon laser line 488 for FITC (B), He-Ne

694   laser 543 for Rhodamine (C) or both. Obtained images show co-localization of Na$^+$/H$^+$
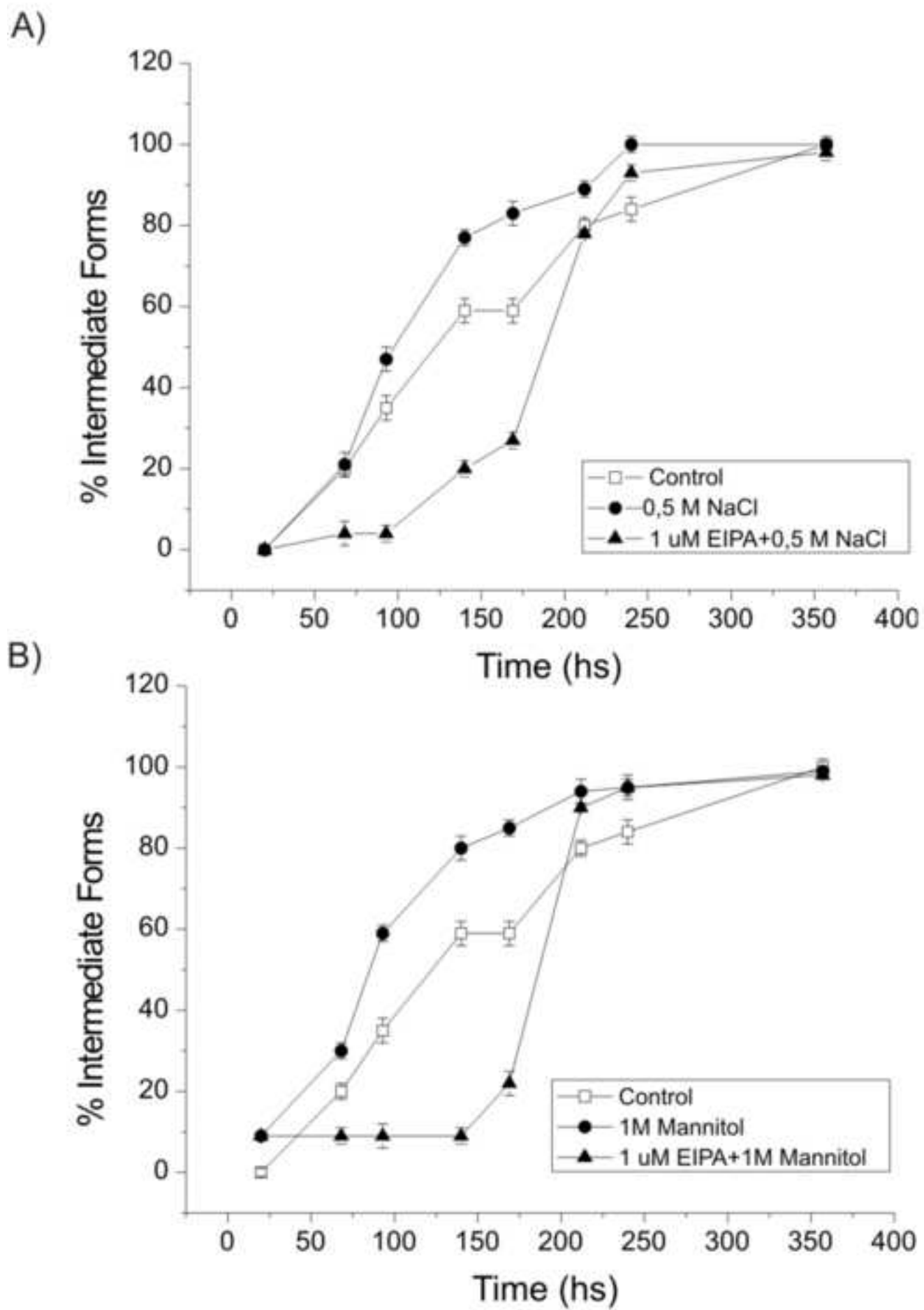
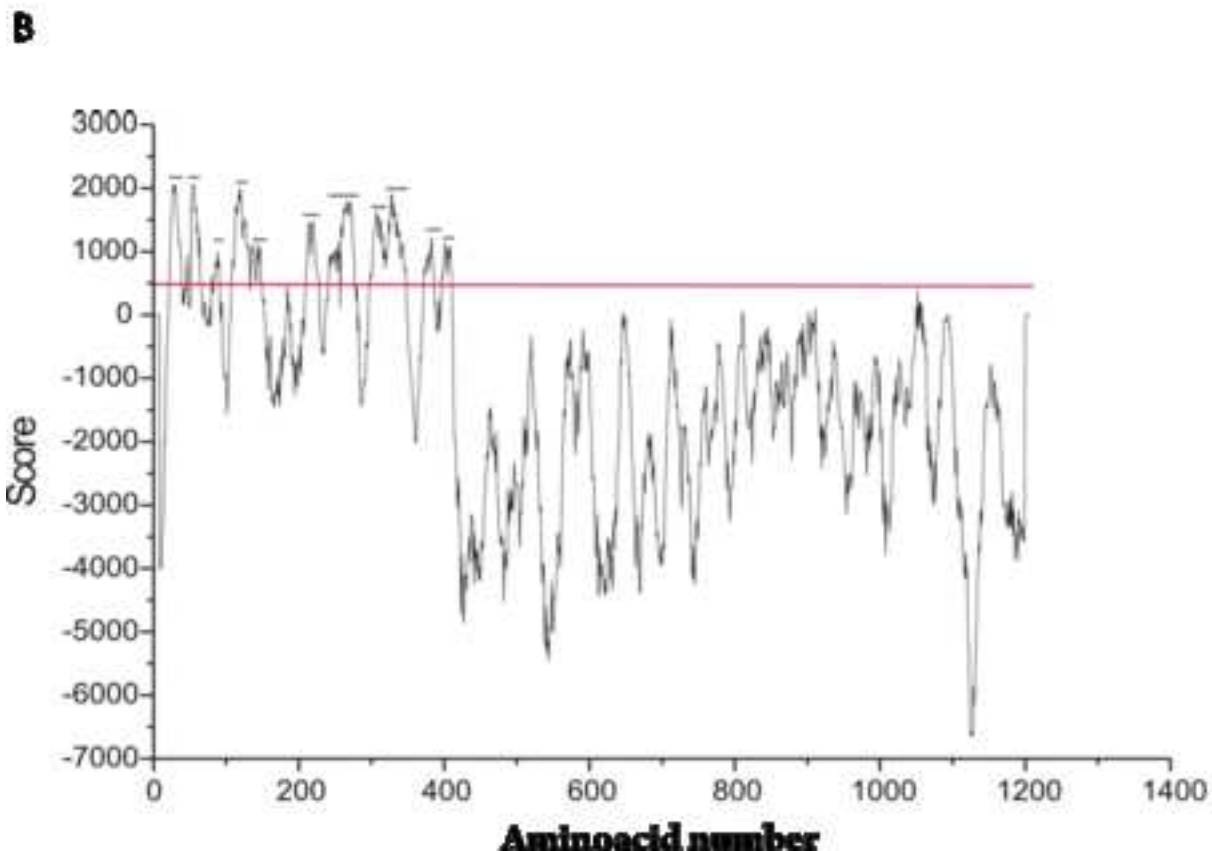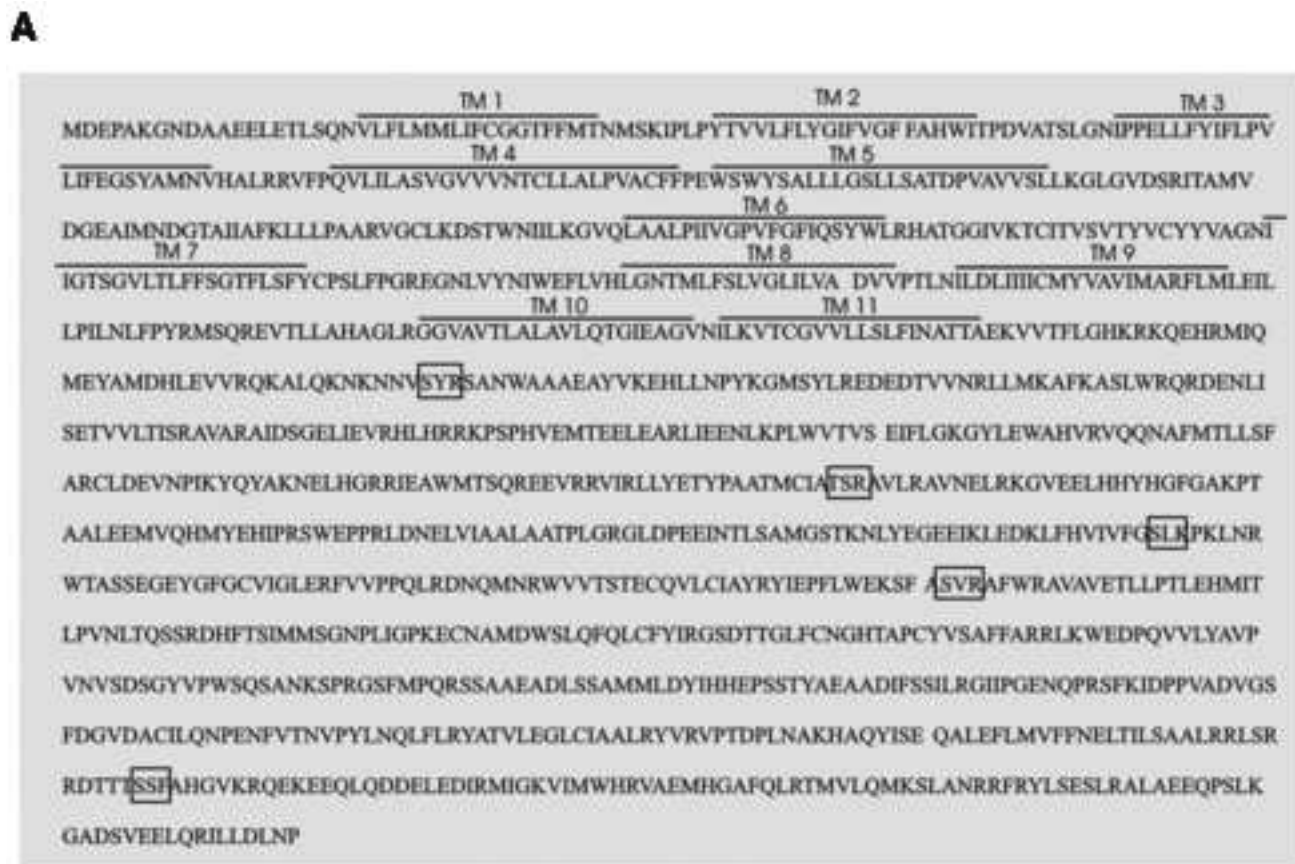695   and V-H$^+$ PPase (D).

Figure 1

Figure 2

Figure 3

Figure 4

Figure 5

A)

B)

Figure 6

Figure 7

Saccharomyces cerevisiae
(NHX1)

Dictyostelium
discoideum

Homo sapiens
(NHE9)

Homo sapiens
(NHE7)

Homo sapiens
(NHE8)

Homo sapiens (NHE6)

Arabipopsis thaliana
(NHX1)

Arabipopsis
thaliana (NHX2)

Oryza sativa
(NHX1)

IC-NHE

Homo sapiens
(NHE3)

Homo sapiens
(NHE5)

Homo sapiens
(NHE1)

Homo sapiens
(NHE2)

Homo sapiens
(NHE4)

98

100

100

PM-NHE

Trypanosoma
cruzi

Leishmania
major

94

100

Toxoplasma gondii
(NHE1)

Plasmodium
falciparum (SOS1)

Arabipopsis thaliana
(NHX8)

Arabipopsis thaliana
(SOS1)

Cymodocea
nodosa (SOS1)

Oryza sativa
(SOS1)

Physcomitrella patens
(SOS1)

Cryptosporidium
parvum (SOS1)

Plasmodium
berghei(SOS1)

Plasmodium
yoelii yoelii
(SOS1)

Plasmodium
chabaudi (SOS1)

Toxoplasma gondii
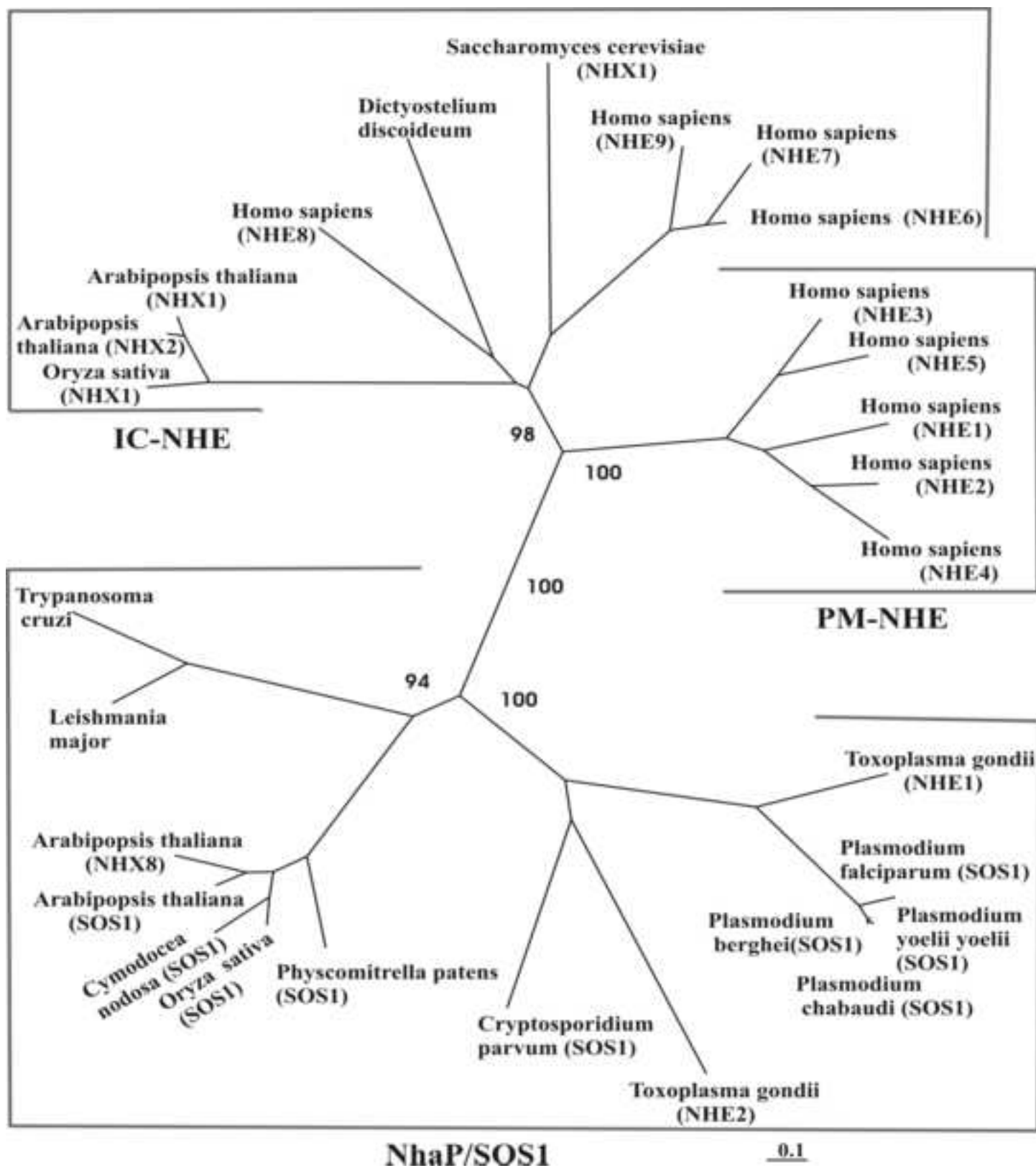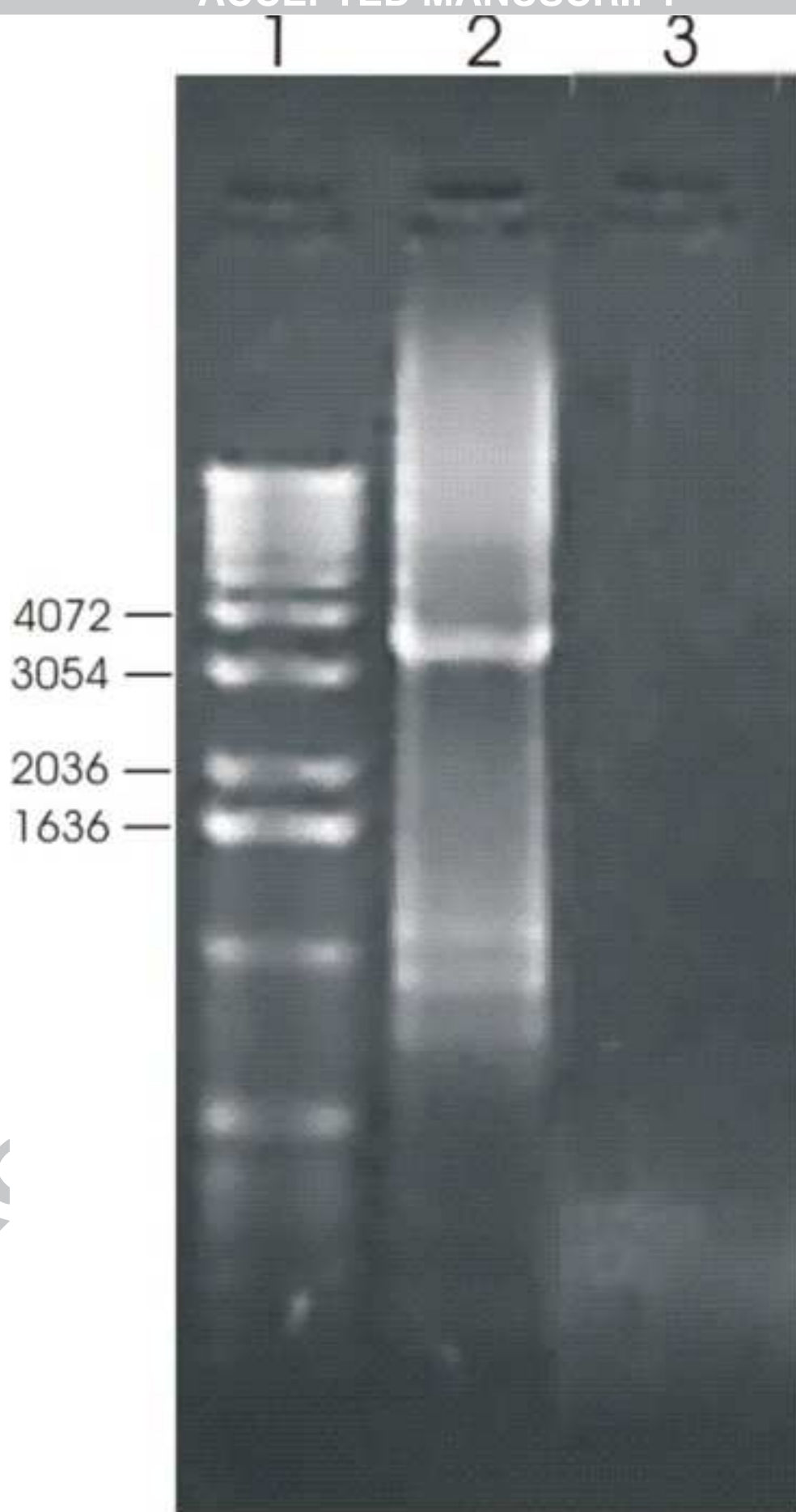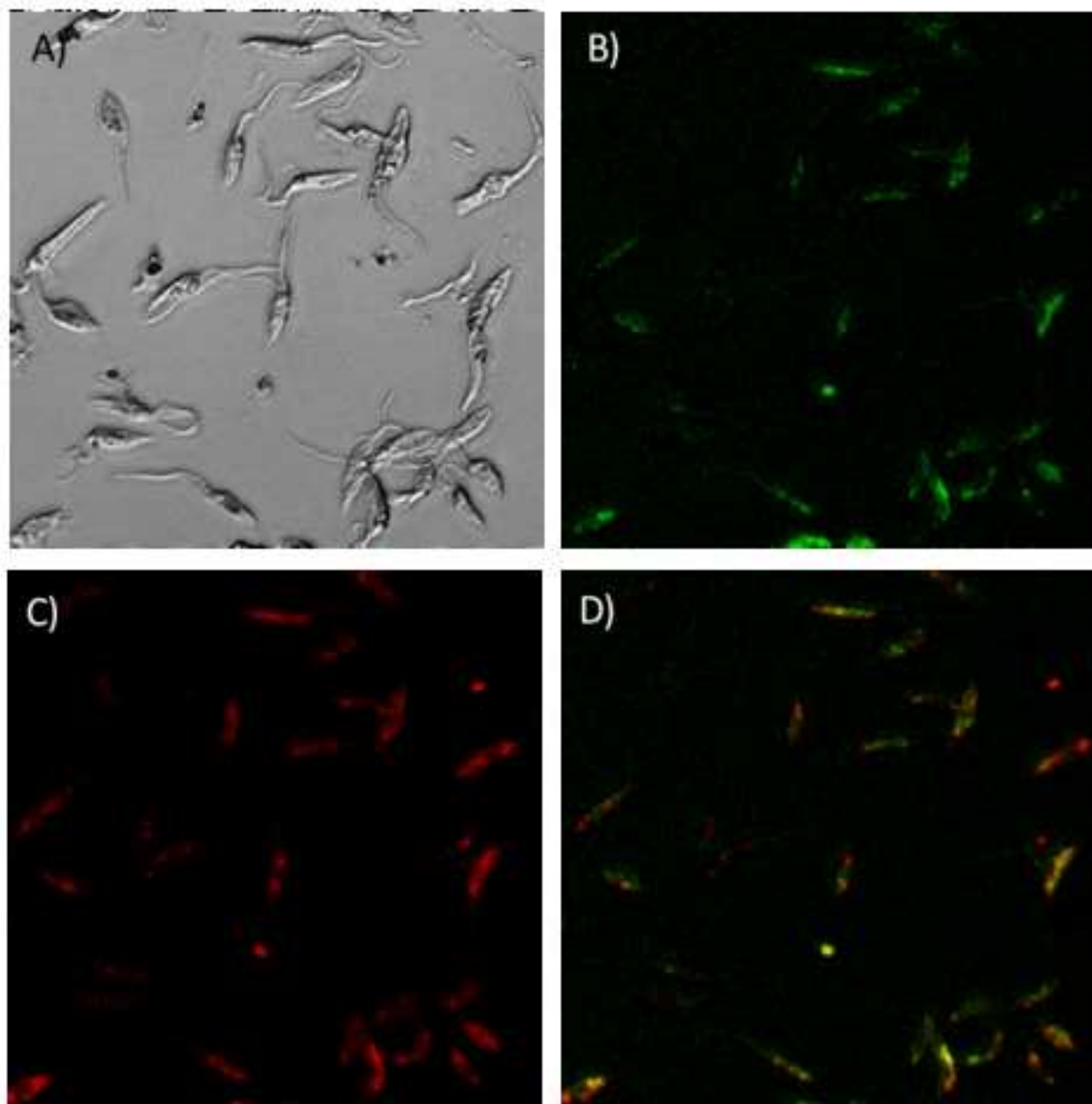(NHE2)

NhaP/SOS1

0.1

Figure 8

Figure 9

696

697 **Table I: Similarity of TcNHE1 to Na$^+$/H$^+$ exchangers.** Amino acidic identity and

698 similarity comparisons between the putative protein and Na$^+$/H$^+$ exchangers from

699 different organisms are shown. Identity and similarity percentages were obtained with

700 BLAST2seq analysis.

701

Species	GenBank Accession Nº	Gene Name	I/S percentages (%)	Expect value (E)
Leishmania major	CAJ04461.1	--	58/78	1E^{-169}
Toxoplasma gondii	AAU81711.1	TgNHE2	25/47	5E^{-24}
Toxoplasma gondii	ADA83376	TgNHE3	22/46	4E^{-16}
Toxoplasma gondii	AAR85890.1	TgNHE1	24/44	9E^{-17}
Plasmodium yoelii yoelii	EAA22449.1	--	22/46	2E^{-25}
Arabidopsis thaliana	NP_178307.2	AtSOS1	28/47	3E^{-56}
Oryza sativa	AAP93587.1	OsSOS1	27/47	3E^{-46}
Pseudomona aeruginosa	BAA31695.1	PaNHAP	28/48	2E^{-16}
Homo sapiens	NP_003038.2	HsNHE1	22/43	2E^{-09}

702

703

704

705

706

707

708

Highlights

Hyperosmotic stress induces alkalinization of acidocalcisomes and calcium release.

High osmolarity induces phospholipase C activation via a Na^+/H^+ exchanger.

T. cruzi Na^+/H^+ antiporter is localized in acidic vacuoles of epimastigotes.

Protein kinase C is involved in vacuolar alkalinization induced by hyperosmolarity.

714

715